Proceedings of the 6th Nordic Signal Processing Symposium - NORSIG 2004
June 9 - 11, 2004
Espoo, Finland

Time Invariant Curvelet Denoising

Birgir Bjorn Saevarsson, Johannes R. Sveinsson and Jon Atli Benediktsson
University of Iceland
Department of Electrical and Computer Engineering
Hjardarhaga 2-6, 107 Reykjavik
ICELAND
E-mail: {birgirsa, sveinsso, benedikt}@hi.is

ABSTRACT

The purpose of this paper is to develop a method for denoising images corrupted with additive white Gaussian noise (AWGN). The noise degrades quality of the images and makes interpretations, analysis and segmentation of images harder. In the paper the use of the time invariant discrete curvelet transform for noise reduction is considered. The discrete curvelet transform is a new image representation approach that codes image edges more efficiently than the wavelet transform. Edges are very important in image perception and with fewer coefficients to represent edges, a better denoising scheme can be achieved. By making the curvelet transform time invariant greatly reduces the energy of the error resulting in better denoising.

1. Introduction

Almost every kind of data contains some kind of noise. For digital images, noise reduction is often a required step for many sophisticated exploring methods such as remote sensing of digital images.
The normal representation of a digital image is a matrix of pixels where each pixel measures the brightness of an object. The pixel values for a normal 8-bit grayscale images lie between 0 and 255.
Denoising is the process of reducing the noise in the digital images. Denoising usually consists of three stages:

1) Transform the noisy image to a new space, i.e., find a representation which discriminates the image from the noise.
2) Manipulate the coefficients in the new space, i.e., keep the coefficient where the signal to noise ratio is high, reduce the coefficient where the signal to noise ratio is low.
3) Transform the manipulated coefficients back to the original space.

In [1], Donoho and Candes proposed the ridgelet transform and showed that it is superior to other denoising methods such as Fourier and wavelet denoising at handling one dimensional discontinuity, i.e., straight edges. Because regular images have curved edges the ridgelet transform is not sufficient to handle linear discontinuities in images. This is why Donoho and Candes proposed the curvelet transform by utilizing the ridgelet transform [2]. Here a time invariant version of the discrete curvelet transform is proposed by implementing cycle spinning on two of the three subbands of the curvelet transform. The biggest problem with image denoising is the edges of images. By performing cycle spinning the largest error of a denoised image is reduced resulting in lower energy of the error which gives better denoising result [3].
The paper is organized as follows. First, in Section 2, the curvelet transform is introduced. The time invariant discrete curvelet transform is discussed in Section 3 and the denoising method is described in Section 4. Experimental results are given in Section 5 and finally, conclusions are drawn in Section 6.

2. CURVELET TRANSFORMATION

The discrete curvelet transform for a 256×256 image is performed as is shown in Fig. 1. As can be seen in Fig. 1 the discrete curvelet transform can be performed in three steps:

1) The 256×256 image is split up in three subbands.
2) Tiling is performed on subbands Δ_1 and Δ_2.
3) Discrete ridgelet transform is performed on each tile.

2.1 Subband Filtering

The subband filtering for a 256×256 image I is done as follows. The image is split up in three subbands $s = 0, 1, 2$ and undecimated discrete wavelet transformation is used to implement the subband filtering. The 6-tap Daubechies undecimated discrete wavelet transform is used [4]. Fig. 2 shows the the relationship between subbands and the frequency domain where $s = 0$ indicates the basis subband, $s = 1$ indicates the bandpass

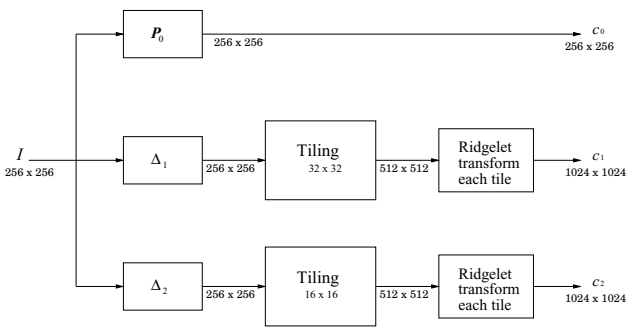

Fig. 1. The flowchart for the discrete curvelet transform.

©2004 NORSIG 2004

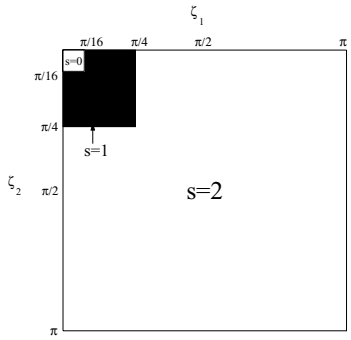

Fig. 2. Subband division for a 256×256 image I.

subband, and $s = 2$ indicates the highpass subband. As an example, the Lena image I is split in the basis subband $P_0 I$, bandpass subband $\Delta_1 I$ and highpass subband $\Delta_2 I$ as shown in Fig. 3. Note that, the relationship between the Lena image I and its subbands is given by

$$I = P_0 I + \Delta_1 I + \Delta_2 I.$$

2.2 Tiling

The ridgelet transform was designed to code linear singularities well but it does not handle curved edges nearly as well [6]. This is why the subbands Δ_1 and Δ_2 are tiled because by zooming well enough into the image, some curved edges will become linear singularities. The tiling for the 256×256 subbands Δ_1 and Δ_2 are decomposed into overlapping blocks of sidelength 32 and 16, respectively. A typical tiling is shown in Fig. 4 where a 64×64 Lena image is zero padded and partitioned into overlapping blocks of sidelength 32. The image is

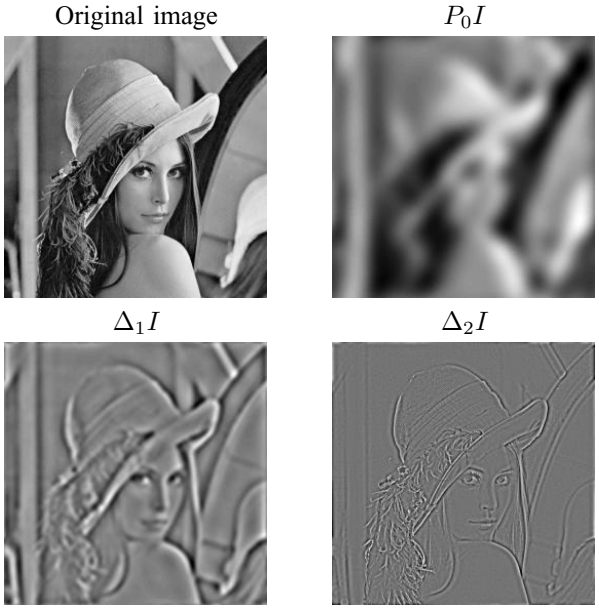

Fig. 3. Lena image I and its subbands.

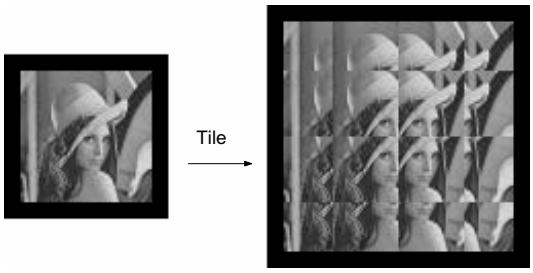

Fig. 4. Tiling of a 64×64 Lena image.

zero padded because every pixel of subbands Δ_1 and Δ_2 must appear in adjacent tiles.

2.3 Ridgelet Transform

The 2-D continuous ridgelet transform in $\mathbf{R}^2$ can be defined as follows. First define a smooth wavelet function $\psi : \mathbf{R} \to \mathbf{R}$ satisfying the admissibility condition given by

$$\int_{-\infty}^{\infty} \frac{|\hat{\psi}(\varepsilon)|^2}{|\varepsilon|^2} d\varepsilon < \infty, \quad (1)$$

where $\hat{\psi}$ is the Fourier transform of ψ. Equation (1) holds if ψ has a vanishing mean, i.e.,

$$\int_{-\infty}^{\infty} \psi(t) dt = 0.$$

The bivariate ridgelet $\psi_{a,b,\theta} : \mathbf{R}^2 \to \mathbf{R}^2$ is defined by

$$\psi_{a,b,\theta}(x,y) = a^{-1/2} \cdot \psi((x\cos(\theta) + y\sin(\theta) - b)/a), \quad (2)$$

and the function is constant along the lines $x\cos(\theta) + y\sin(\theta) = \text{const}$. The ridgelet values for continuous image $f(x,y)$ is given by

$$\mathcal{R}f(a,b,\theta) = \int\int f(x,y)\psi_{a,b,\theta}(x,y)dxdy. \quad (3)$$

The Radon transform in continuous terms is defined by

$$Rf(t,\theta) = \int f(x,y)\delta(t - x\cos(\theta) - y\sin(\theta))dxdy, \quad (4)$$

where δ denotes the Dirac delta-function. In words, Rf is the integral of the continuous image f, over the line $L_{t,\theta}$ defined by $t = x\cos(\theta) + y\sin(\theta)$. Parameters t and θ are described in Fig. 5. In short, the ridgelet transform is the application of a 1-D wavelet transform to the slice of the Radon transform where the angular variable θ is constant and t is varying [1]. This means the ridgelet coefficients $\mathcal{R}f(a,b,\theta)$ are given by analysis of the Radon transform via

$$\mathcal{R}f(t,\theta) = \int Rf(t,\theta)a^{-1/2}\psi((t-b)/a)dt, \quad (5)$$

where $\psi_{a,b}(t) = a^{-1/2}\psi((t-b)/a)$ is a 1-D wavelet. The flowchart for the ridgelet transform can be seen in Fig. 6. Since the images used are discrete but not continuous the ridgelet transform has to be discrete. To make the ridgelet transform discrete the Radon transform as well

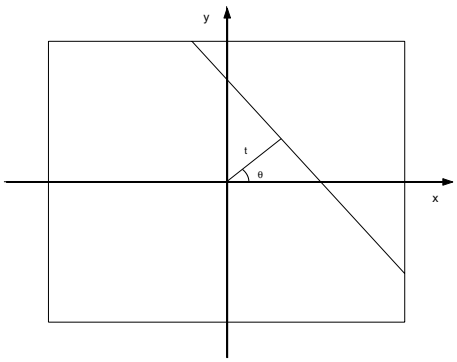

Fig. 5. Radon parameters defined. The frame indicates the image, and the line, $L_{t,\theta}$, indicates area that we need to integrate to get a single Radon coefficients.

as the wavelet transform have to be discrete. The discrete wavelet transform is well defined but the same can not be said about the discrete Radon transform. There are many ways to make the Radon transform discrete and in this paper a fast method is used, given in [5].

3. TIME INVARIANT DISCRETE CURVELET TRANSFORM

For the discrete curvelet transform to be time invariant a 2-D cycle spinning is implemented on subbands Δ_1 and Δ_2. A framework for 1-D cycle spinning is shown in Fig. 7. The data is shifted, denoised and unshifted. For the discrete curvelet transform the shift length of rows and columns, depends on the block size. For the discrete curvelet transform to be completely time invariant, subbands Δ_1 and Δ_2 need to be shifted by $b/2-1$ for both rows and columns where b stands for sidelength. This means the total number of shifts required is $b^2/4-b+1$, which means subband Δ_2 with $b=16$ requires 49 shifts and subband Δ_1 with $b=32$ requires 225 shifts. The reason for why the cycle spinning is performed is to try to find all $b\times b$ blocks that contain linear singularities.

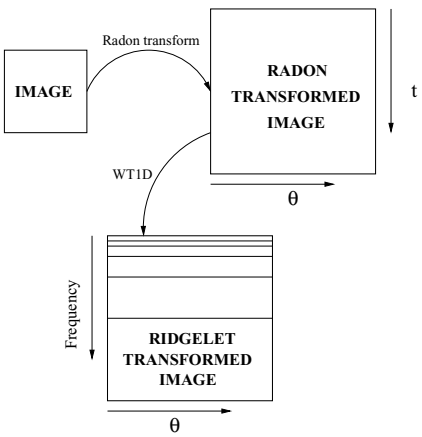

Fig. 6. Flowchart for the ridgelet transformation. First the image is Radon transformed, and then 1-D wavelet transform (WT1D) is performed on the Radon transformed image.

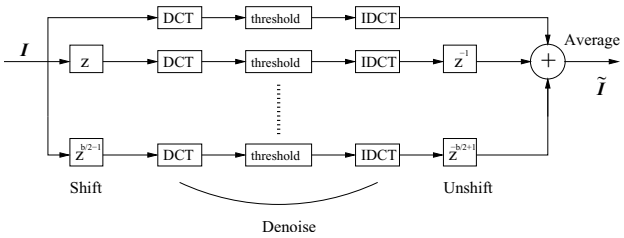

Fig. 7. Framework of the cycle spinn denoising algorithm. Here DCT stands for discrete curvelet transform and b stands for sidelength.

4. DENOISING METHODS

Since the discrete curvelet transform is not norm-preserving, the variance of each curvelet coefficient depends on its index [6]. Let C denote the discrete curvelet transformation matrix and curvelet transform an image with noise distribution given by $\mathcal{N}(0,1)$, then the outcome has noise distribution given by $\mathcal{N}(0,CC^*)$. To estimate the noise variance of each curvelet index, the Monte-Carlo simulation method is used. Few standard white noise images, I, with zero mean and variance one, i.e., $\mathcal{N}(0,1)$ were discrete curvelet transformed and the variance, $\tilde{\sigma}_\lambda^2$ was estimated where λ indicates its index. The denoising algorithm for time variant and time invariant curvelet transform is performed by thresholding the curvelet coefficients c with

$$\tilde{c}_\lambda = \begin{cases} c_\lambda & |c_\lambda| \geq k\tilde{\sigma}_\lambda\sigma \\ 0 & |c_\lambda| < k\tilde{\sigma}_\lambda\sigma, \end{cases} \tag{6}$$

where σ is estimation of the standard deviation of the noise of image I and k is subband dependent value, estimated by denoising few known images and letting k variate.

5. EXPERIMENTAL RESULTS

The value for the subbands were estimated as $k=2.6$ for subband Δ_1 and $k=9.2$ for subband Δ_2. A 256×256, 8-bit grayscale Lena image, with the pixel values of the image scaled to the interval $[0,1]$ is going to be used in this experiment. Gaussian white noise $\mathbf{n}$ with standard deviation $\sigma=0.1$ is added to the image I and the outcome is

$$Y[u,v] = I[u,v] + \sigma n[u,v] \quad 0\leq u,v\leq 255. \tag{7}$$

The noisy image Y was then denoised with both time variant and time invariant discrete curvelet transform using the hard threshold given by (6). Three methods where used to estimate the quality of the denoising methods called peak signal-to-noise ratio (PSNR), equivalent number of looks (ENL) and edge strength index (ESI). The PSNR is given by

$$\text{PSNR} = 10\cdot\log\frac{(\text{p-to-p value of the reference image})^2}{\sigma_e^2}, \tag{8}$$

where p-to-p stands for peak to peak and the mean

(a) (b) (c)

Fig. 8. (a) Noisy Lena image. (b) Lena image denoised by using the discrete curvelet transform. (c) Lena image denoised by using the time invariant disctete curvelet transform.

squared error σ_e^2 is given by

$$\sigma_e^2 = \frac{1}{MN} \sum_{m=1}^{M} \sum_{n=1}^{N} |I[m,n] - \tilde{I}[m,n]|^2. \qquad (9)$$

Here I is the original image and $\tilde{I}$ is the denoised image. The ENL method is used to estimate how well homogeneous regions of the noisy images are denoised. The ENL value is calculated by

$$\text{ENL} = \frac{(\text{mean})^2}{\text{variance}}, \qquad (10)$$

where the mean and the variance are calculated for a small homogeneous region of an image as shown in Fig. 9. A large value of the ENL indicates good denoising of the homogeneous region. The ESI is given by

$$\text{ESI} = \frac{\sum_{i=1}^{m} |R_1[i] - R_2[i]|_{\text{denoised}}}{\sum_{i=1}^{m} |R_1[i] - R_2[i]|_{\text{original}}}, \qquad (11)$$

where $\{R_1[i], R_2[i]\}$, $i = 1, 2, ..., m$ are pairs of neighboring pixels where $R_1[i]$ and $R_2[i]$ are on the edge of Lena's hat as shown by white stripes in Fig. 9. The experimental results are shown in Table 1 and in Fig. 8.

Fig. 9. Parts of the Lena image used to calculate the ENL and ESI values. The rectangular area is used to calculate the ENL value and the white stripes on the edge of Lena's hat are used to calculate the ESI value.

Table 1. PSNR, ENL and ESI results for experiments on the Lena image using 30 iteration. Here DCT denotes discrete curvelet transform and TIDCT denotes time invariant discrete curvelet transform.

Methods	PSNR (dB)	ENL	ESI
Noisy image	20.00	28.67	1.01
DCT	27.18	450.50	0.84
TIDCT	28.16	636.55	0.86

6. CONCLUSION

The time invariant curvelet transform denoising for 256×256 images was proposed and compared with the regular curvelet transform denoising methods. Both methods significantly reduce the AWGN while preserving the resolution and the structure of the original images as is shown in Fig. 8. Experimental results given in Table 1 show that the time invariant transform outperforms the time variant transform in all three estimations giving a good and clean image, which should improve classification and recognition.

REFERENCES

[1] E.J. Candes, *Ridgelets: Theory and Applications*, PhD thesis, Stanford University, 1998.

[2] E.J. Candes and D.L Donoho, "Curvelets - a surprisingly effective nonadaptive representation for objects with edges," in *Curve and Surface Fitting: Saint-Malo 1999*, (A. Cohen and C. Rabut and L. L. Schumaker, eds.), 1999.

[3] R.R. Coifman and D.L. Donoho, "Translation-Invariant Denoising," *Wavelets and Statistics*, Springer Lecture notes in Statistics 103, pp. 125–150, New York: Springer-Verlag, 1995.

[4] H. Guo, "Theory and Application of The Shift-Invariant, Time-Varying and Undecimated Wavelet Transform," Master's thesis, Rice University, 1995.

[5] A. Averbuch, R.R. Coifman, D.L. Donoho, M. Israeli, J. Walden, "Fast Slant Stack: A notion of Radon Transform for Data in a Cartesian Grid which is Rapidly Computible, Algebraically Exact Geometrically Faithful and Invertible," 2001. Available: http://www-stat.stanford.edu/˜donoho/reports.html.

[6] J. Starck, E.J. Candes, and D.L. Donoho, "The Curvelet Transform for Image Denoising," *IEEE Transaction on Image Processing*, vol. 11, no. 6, pp. 670–684, 2001.